

# Micro and macroscopic models of rock fracture

Donald L. Turcotte,<sup>1,3</sup> William I. Newman<sup>2,3</sup> and Robert Shcherbakov<sup>1,3</sup>

<sup>1</sup>Department of Earth and Atmospheric Sciences, Snee Hall, Cornell University, Ithaca, NY 14853, USA.

E-mails: turcotte@geology.cornell.edu; roshch@geology.cornell.edu

<sup>2</sup>Departments of Earth & Space Sciences, Physics & Astronomy, and Mathematics, University of California, Los Angeles, CA 90095, USA.

E-mail: win@ucla.edu

<sup>3</sup>Institute for Mathematics and its Applications Lind Hall, University of Minnesota, Minneapolis, MN 55455, USA

Accepted 2002 October 2. Received 2002 October 1; in original form 2002 March 1

## SUMMARY

The anelastic deformation of solids is often treated using continuum damage mechanics. An alternative approach to the brittle failure of a solid is provided by the discrete fibre-bundle model. Here we show that the continuum damage model can give exactly the same solution for material failure as the fibre-bundle model. We compare both models with laboratory experiments on the time-dependent failure of chipboard and fibreglass. The power-law scaling obtained in both models and in the experiments is consistent with the power-law seismic activation observed prior to some earthquakes.

**Key words:** critical point, damage mechanics, fibre-bundle model, fracture, power-law scaling.

## 1 INTRODUCTION

The brittle failure of a material is a complicated phenomenon. For example, it can involve a single fracture propagating through a homogeneous solid. However, this is an idealized case that requires a pre-existing crack or notch to concentrate the applied stress. The propagation of the fracture is not fully understood because of the complexities of the stress singularities at the crack tip (Freund 1990). In general, the initiation of a fracture in a solid is a more complex process. Even if the material appears to be homogeneous, there will be a distribution of dislocations, flaws, and other heterogeneities present. As the applied stress is increased, microcracks occur randomly on the heterogeneities and are uncorrelated. As the density of microcracks increases the stress fields of the microcracks interact and the microcracks become correlated. The microcracks eventually coalesce to form a through-going fracture. This irreversible process is a part of damage mechanics.

Many experiments on the fracture of rocks and other brittle materials have been carried out. Mogi (1962) monitored the acoustic emissions from the microcracks in rock and showed that they satisfied power-law frequency–magnitude statistics. He also showed that there was a well-defined delay between the application of a constant stress and the failure of the rock. Hirata *et al.* (1987) showed that the acoustic emissions prior to the failure of a rock satisfied a power-law (fractal) spatial distribution. Similar results were obtained by Lockner (1993).

Many authors have studied the time delays associated with brittle failure after a constant stress has been applied to a brittle solid. Similar experiments were conducted by Zhurkov (1965) for brittle fracture of a wide variety of materials. Otani *et al.* (1991) obtained the statistical distribution of delay times for failure after the appli-

cation of a constant stress to carbon fibre–epoxy microcomposites. Anifrani *et al.* (1995) and Johansen & Sornette (2000) studied the rupture of spherical tanks of kevlar wrapped around thin metallic liners and found a power-law increase of acoustic emissions prior to rupture. Guarino *et al.* (1998, 1999) studied the failure of chipboard and fibreglass panels. They also found a power-law increase in acoustic emissions prior to failure and a systematic dependence of failure times on the stress level.

In terms of the Earth's crust, brittle failure generally occurs on pre-existing faults, and the applicable process is assumed to be friction. The fault fails when the applied shear stress exceeds that produced by a static coefficient of friction. During rupture the stress on the fault is given by the dynamic coefficient of friction. As long as the dynamic coefficient of friction is less than the static coefficient of friction, stick-slip behaviour results and there are earthquakes. Many papers have considered the failure of one or more specific planar faults in a homogeneous elastic medium (Ben-Zion & Rice 1995). However, the Earth's crust is made up of faults on all scales that interact. One consequence of these interactions is the scale invariant Gutenberg–Richter frequency–magnitude relation for earthquakes. Evidently, the Earth's crust is a self-organizing complex medium.

While there are important similarities between the fracture of a pristine rock and an earthquake rupture, there are also important differences. The fracture of a pristine rock is an irreversible process. However, earthquake ruptures occur repetitively on pre-existing faults and, between earthquakes, faults heal. If the Earth's crust, prior to a major earthquake, behaved as the fracture of a pristine rock, there would be a systematic increase in regional seismicity before a major earthquake. The rate of occurrence of small earthquakes in a seismogenic zone is nearly constant (Turcotte 1999). However, there is accumulating evidence that there is an increase in

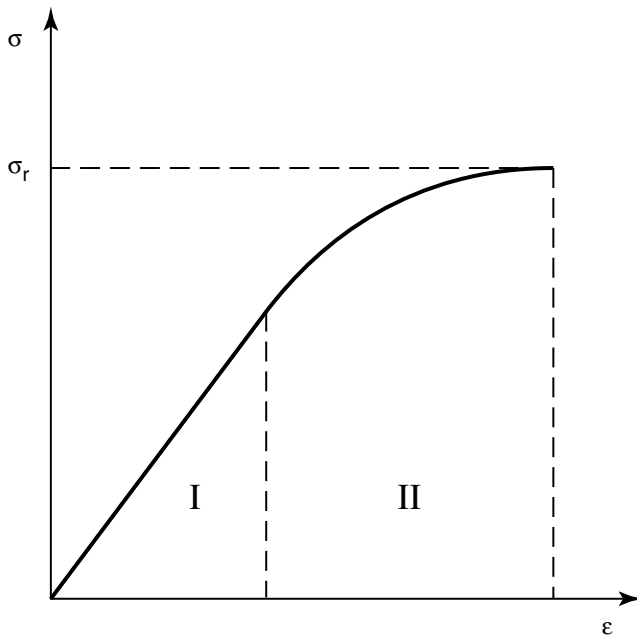


**Figure 1.** A schematic illustration of the failure of a brittle rod. In region I, linear elasticity is applicable. In region II, damage is occurring and there is irreversible deformation of the rod.

the number of intermediate-sized earthquakes prior to a large earthquake (Rundle *et al.* 2000). The repetitive nature of earthquakes, and their power-law scaling, have led some authors to argue that seismicity is an example of self-organized criticality (Bak & Tang 1989). It is certainly reasonable to hypothesize that the Earth’s crust is in a ‘damaged’ state. Evidence of this damage is the continuous occurrence of small earthquakes that satisfy Gutenberg–Richter frequency–magnitude scaling.

In this paper we will consider both microscopic and continuum models of damage. We will compare both types of models with laboratory experiments and will discuss the implications for earthquake physics. The behaviour of a rod of material under tension is illustrated schematically in Fig. 1. Deviations from linear elasticity and the existence of damage are shown schematically. The stress  $\sigma$  in the rod is given as a function of the strain  $\epsilon$ . In region I, linear elasticity is applicable and we have

$$\sigma = E_0 \epsilon, \tag{1.1}$$

where  $E_0$  is the Young modulus of the undamaged material, a constant. In region II, where there is a deviation from linear elasticity, microcracking is occurring. These microcracks weaken the material and result in acoustic emissions. For a prescribed stress  $\sigma$ , the strain  $\epsilon$  is greater than the value given by eq. (1.1). Accordingly, we write

$$\sigma = E_{\text{eff}} \epsilon, \tag{1.2}$$

where  $E_{\text{eff}}$  is the effective Young modulus—it is no longer assumed to be a constant. This relation between  $\sigma$  and  $\epsilon$  provides the definition of  $E_{\text{eff}}$ .

A continuum approach to this process is to introduce a damage variable  $\alpha$  so that (Kachanov 1986; Lemaitre & Chaboche 1990; Lyakhovskiy *et al.* 1993, 1997; Krajcinovic 1996)

$$E_{\text{eff}} = E_0 (1 - \alpha). \tag{1.3}$$

The damage variable  $\alpha$  quantifies the deviation from linear elasticity and the distribution of microcracks in the 1-D problem. In general

$0 \leq \alpha \leq 1$ . When  $\alpha = 0$ , linear elasticity is obtained with eq. (1.1) valid, but when  $\alpha = 1$ , failure occurs. For quasistatic (slow) rupture it is appropriate to take the damage variable to be a function only of the applied stress  $\alpha(\sigma)$ . However, in most cases of interest the development of damage in a material is a transient process so that we have  $\alpha[\sigma(t)]$ . As illustrated in Fig. 1, the failure of the brittle material occurs at  $t = t_f$  when  $\sigma(t_f) = \sigma_r$  ( $\alpha = 1$ ), the failure stress. It should be emphasized that the dependence given in Fig. 1 is highly idealized since the dependence on time is not illustrated.

Another approach to brittle failure is applicable to composite materials. A composite material is made up of strong fibres embedded in a relatively weak matrix. Failure of composite materials has been treated by many authors using the concept of fibre-bundles (Smith & Phoenix 1981; Curtin 1991; Newman & Phoenix 2001). The failure statistics of the individual fibres that make up the fibre-bundle are specified. The statistics can be either static or dynamic. In the static case, the probability of the failure of a fibre is specified in terms of the stress on the fibre. Failure is assumed to occur instantaneously. In the dynamic case, the statistical distribution of times to failure for the fibres are specified in terms of the stresses on the fibres (Coleman 1956, 1958). Experiments generally favour the dynamic-failure, fibre-bundle models. When stress is applied to a fibre-bundle, the fibres begin to fail. It is necessary to specify how the stress on a failed fibre is redistributed to the remaining sound fibres (Smith & Phoenix 1981). In the uniform load sharing hypothesis, the stress from a failed fibre is redistributed equally to the remaining fibres. This is a mean-field approximation. The alternative redistribution model is the local load sharing hypothesis. In this case the load on the failed fibre is redistributed to neighbouring fibres. Local load sharing is applicable to strongly bonded fibrous (composite) materials, whereas equal load sharing is applicable to weakly bonded fibrous materials.

The failure of a simple fibre-bundle under uniform load sharing is illustrated in Fig. 2. Initially the load on the bundle  $F_0$  is carried equally by the four fibres with  $F = \frac{1}{4}F_0$ . The weakest fibre fails and the load on that fibre is now carried by the surviving fibres with  $F = \frac{1}{3}F_0$ . The stress on each fibre increases from the original value  $\sigma_0$  to  $\frac{4}{3}\sigma_0$ . The process of failure followed by stress redistribution continues until all fibres fail and no load can be carried. The fibre-bundle model can also be used as a simple model for friction where the fibres represent the asperities on a surface.

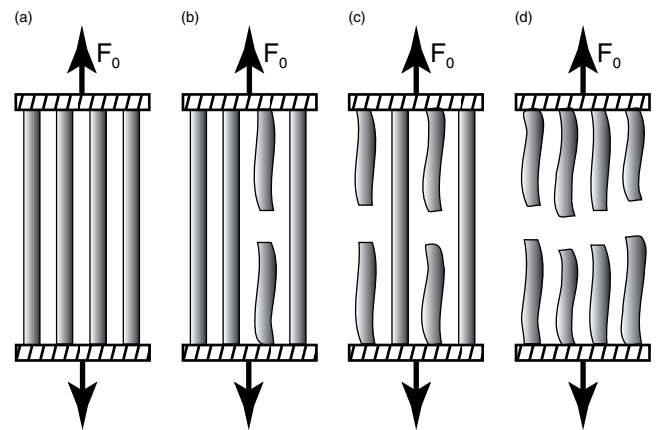


**Figure 2.** A schematic illustration of the failure of a fibre-bundle with uniform load sharing. (a) Each of the fibres carries one-quarter of the load  $F_0$ . (b) One fibre has failed and each remaining fibre carries one-third of the load  $F_0$ . (c) Two fibres have failed and each remaining fibre carries one-half of the load  $F_0$ . (d) All four fibres have failed and no load is carried.

The primary purpose of this paper is to compare the microscopic fibre-bundle model for failure with the macroscopic damage model for failure in a simple geometry. We consider the two models for the failure of a rod under tension. The dynamic fibre-bundle model is considered assuming uniform load sharing. The rate of failure of fibres under an initial stress  $\sigma_0$  (per fibre) is specified. As fibres fail, the stress on the remaining fibres increases leading to a catastrophic failure of the bundle. The fibre failures are equivalent to the microcracks that occur in a uniform brittle material as it is stressed to failure.

The second model we consider for the failure of a rod is the continuum damage model. A damage variable  $\alpha$  is introduced as in eq. (1.3). Based on thermodynamic considerations, an expression is introduced for the increase in the damage variable with time. When  $\alpha = 1$ , catastrophic failure of the rod occurs. This analysis was previously carried out by Ben-Zion & Lyakhovsky (2002).

We obtain solutions for two initial-value problems. In the first problem, a constant force  $F_0$  is applied instantaneously at  $t = 0$ . The time to failure  $t_f$  is determined. In the second problem we assume that the applied force  $F(t)$  is increased linearly with time  $F(t) \propto t$  until failure occurs. We show that the two models can give identical algebraic forms for the solutions of these problems. Moreover, these solutions correspond to the constant applied force problem, when the time variable is suitably scaled. The damage variable  $\alpha$  is given by the fraction of fibres that fail, namely  $\alpha = 1 - N/N_0$ , where  $N_0$  is the original number of fibres in the bundle and  $N$  is the number of remaining fibres. A qualitative discussion of the relation between the fibre-bundle model and the continuum damage model has been given previously by Krajcinovic (1996).

A characteristic of material failure is the emergence of acoustic-emission events. The acoustic-emission events are generated by microcracks as the material is damaged. The microscopic fibre-bundle model can be used to obtain the predicted rate of acoustic-emission events prior to material failure. The predictions are compared with the experimental observations of Guarino *et al.* (1998, 1999). These authors determined the rate of acoustic-emission events generated during the failure of panels of chipboard and fibreglass. Their results agree with the predictions of the microscopic fibre-bundle model. We conclude by exploring the possible relevance of these models to seismic activation, and discuss the broader implications of these results.

## 2 FIBRE-BUNDLE MODEL

We consider a rod that is made up of  $N_0$  fibres. This rod can be thought of as a frictionless, stranded cable made up of  $N_0$  strands. The standard approach to the dynamic time-dependent failure of a fibre-bundle is to specify an expression for the rate of failure of fibres (Coleman 1956, 1958; Newman & Phoenix 2001). The form of this breakdown rule is given by

$$\frac{dN(t)}{dt} = -\nu(\sigma_f) N(t), \quad (2.1)$$

where  $N(t)$  is the number of unbroken fibres at time  $t$ , and  $\nu(\sigma_f)$  is known as the hazard rate, which is a function of the fibre stress  $\sigma_f(t)$ .

First we consider the case in which a uniform strain  $\epsilon_0$  is applied to and maintained upon the fibre-bundle at time  $t = 0$ . In this case the stress on each fibre has a constant value  $\sigma_0$  given by eq. (1.1), where  $E_0$  is the Young modulus of a fibre. Since the stress on the fibres is constant, so is the hazard rate, yielding  $\nu = \nu_0$  independent of time  $t$ . In this case eq. (2.1) can be integrated to give

$$\frac{N(t)}{N_0} = e^{-\nu_0 t}, \quad (2.2)$$

where the initial conditions  $N(0) = N_0$  has been used. The total force  $F(t)$  carried by the fibre-bundle at time  $t$  is given by

$$F(t) = N(t) \sigma_0 a, \quad (2.3)$$

where  $a$  is the area of a fibre. Substituting eqs (1.1) and (2.1) into eq. (2.2) gives

$$F(t) = N_0 a E_0 \epsilon_0 e^{-\nu_0 t}. \quad (2.4)$$

The force on the fibre-bundle decreases as fibres fail and catastrophic failure in a finite time does not occur.

We now consider the case in which a constant tensional force  $F_0$  is applied to the fibre-bundle at time  $t = 0$ . The initial stress on each fibre at  $t = 0$ ,  $\sigma_0$ , is given by

$$\sigma_0 = \frac{F_0}{N_0 a}. \quad (2.5)$$

The applied tensional force  $F_0$  remains constant, so that when a fibre fails the force carried by that fibre is redistributed to other fibres. Thus the stress on surviving fibres increases with time. We make the further assumption that the force on a failed fibre is redistributed equally to the remaining fibres. This is uniform load sharing and is a mean-field approximation. One implication of this assumption is that all the remaining fibres have the same stress  $\sigma_f(t)$ . The stress on the surviving fibres is related to the number of sound fibres  $N(t)$  by

$$\sigma_f(t) = \frac{N_0}{N(t)} \sigma_0. \quad (2.6)$$

In order to complete the specification of the problem, it is necessary to prescribe the dependence of the hazard rate  $\nu$  on the stress  $\sigma_f$ . For engineering materials it is standard practice (Newman & Phoenix 2001) to empirically assume the power-law relation

$$\nu(t) = \nu_0 \left[ \frac{\sigma_f(t)}{\sigma_0} \right]^\rho, \quad (2.7)$$

where  $\nu_0$  is the hazard rate corresponding to the initial fibre stress  $\sigma_0$ . It is found experimentally that values of  $\rho$  are in the range 2–5 for various fibrous materials.

Substitution of eqs (2.6) and (2.7) into eq. (2.1) gives

$$\frac{dN(t)}{dt} = -\frac{\nu_0 N_0^\rho}{[N(t)]^{\rho-1}}. \quad (2.8)$$

Integration with the initial condition  $N(0) = N_0$  gives

$$N(t) = N_0 (1 - \rho \nu_0 t)^{1/\rho}. \quad (2.9)$$

Failure of a fibre-bundle occurs when  $N(t_f) = 0$ , the time to failure  $t_f$  is given by

$$t_f = \frac{1}{\rho \nu_0}. \quad (2.10)$$

The stress in each of the remaining fibres at time  $t$  is obtained by substituting eq. (2.9) into eq. (2.6) with the result

$$\sigma_f(t) = \frac{\sigma_0}{(1 - \rho \nu_0 t)^{1/\rho}}. \quad (2.11)$$

Next we determine the strain on the fibre-bundle as failure occurs. We make the assumption that each fibre satisfies linear elasticity until it fails, thus we can write

$$\epsilon_f(t) = \frac{\sigma_f(t)}{E_0}, \quad (2.12)$$

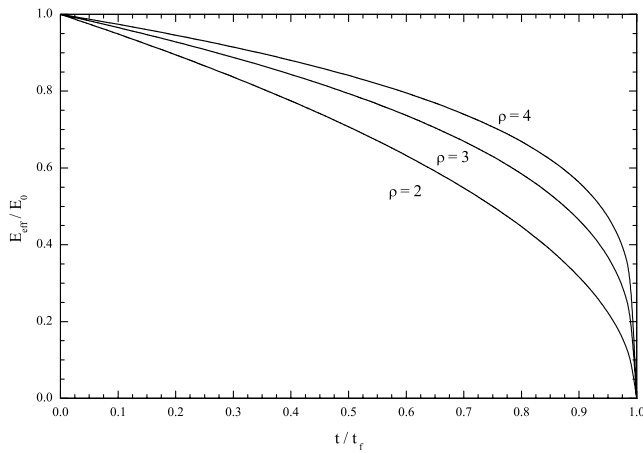


**Figure 3.** Dependence of the ratio of the effective Young modulus  $E_{\text{eff}}$  to the Young modulus of the undamaged material  $E_0$  on the time to failure  $t/t_f$  for  $\rho = 2-4$  from eq. (2.16). A constant force has been applied to the rod at  $t = 0$  and failure occurs at  $t = t_f$ .

where  $E_0$  is the Young modulus applicable to all fibres up to failure. We assume that a microcrack in a fibre results in its failure, i.e. there is no ‘damage’ in a fibre prior to failure. Since the stresses in the remaining fibres are equal with the value  $\sigma_f(t)$ , the strains are also equal with the value  $\epsilon_f(t)$ .

Substitution of eq. (2.11) into eq. (2.12) gives the strain  $\epsilon_f(t)$  of each remaining fibre

$$\epsilon_f(t) = \frac{\sigma_0}{E_0} \frac{1}{(1 - \rho v_0 t)^{1/\rho}}. \tag{2.13}$$

We define an effective Young modulus  $E_{\text{eff}}(t)$  for the fibre-bundle from eq. (1.2) according to

$$E_{\text{eff}}(t) = \frac{\sigma_0}{\epsilon_f(t)}. \tag{2.14}$$

This is the Young modulus of the bundle as a whole (including both failed and sound fibres) treated as an equivalent rod failing under tension. Substitution of eq. (2.13) into eq. (2.14) gives

$$E_{\text{eff}}(t) = E_0(1 - \rho v_0 t)^{1/\rho}. \tag{2.15}$$

Using eq. (2.10) for the time to failure  $t_f$ , we obtain

$$E_{\text{eff}}(t) = E_0 \left(1 - \frac{t}{t_f}\right)^{1/\rho}. \tag{2.16}$$

The effective Young modulus  $E_{\text{eff}}(t)$  decreases from its original value of  $E_{\text{eff}}(0) = E_0$  to  $E_{\text{eff}}(t_f) = 0$  at failure. This dependence is illustrated in Fig. 3 for  $\rho = 2-4$ .

Using eq. (2.9), one can also rewrite eq. (2.15) in the form

$$E_{\text{eff}}(t) = E_0 \frac{N(t)}{N_0}. \tag{2.17}$$

The effective Young modulus  $E_{\text{eff}}(t)$  is linearly proportional to the fraction of fibres that remain unbroken. We have obtained the time-dependent failure of a fibre-bundle to which a constant force  $F_0$  was applied at  $t = 0$ . Next we obtain a solution to the same problem using the damage model.

### 3 DAMAGE MODEL

We have obtained a solution for the strain and effective Young modulus during the failure of a fibre-bundle under a constant applied

load. This was basically a microscopic model in a mean field. We now obtain a solution to the same problem utilizing the macroscopic damage model. Again we consider the failure of a rod under tension. A constant tensional force  $F_0$  is applied to the rod at time  $t = 0$ .

The damage variable  $\alpha$  has been defined in eq. (1.3). Equating eqs (1.3) and (2.17) we obtain

$$\alpha(t) = 1 - \frac{N(t)}{N_0}. \tag{3.1}$$

This definition of damage has been used previously (Krajcinovic 1996). In our analogue with the fibre-bundle model, we can interpret the macroscopic damage variable  $\alpha(t)$  to be the fraction of fibres that have failed. We now determine the time history of strain in a rod using the damage model. We assume that  $\sigma_0$  is the constant stress applied to the rod at  $t = 0$ . For the undamaged material  $\alpha = 0$  and  $E_{\text{eff}} = E_0$ , failure occurs when  $\alpha(t_f) = 1$  and  $E_{\text{eff}}(t_f) = 0$ . Based on thermodynamic considerations (Lyakhovsky *et al.* 1997), the time evolution of the damage variable can be related to the strain  $\epsilon(t)$  by

$$\frac{d\alpha(t)}{dt} = A \epsilon^2(t) \tag{3.2}$$

where  $A$  is a constant for a constantly applied stress. It is assumed that the rate of damage can be expanded in a power-series expansion in  $\epsilon$ . The first power in  $\epsilon$  disappears since we assume that equilibrium is maintained in the thermodynamic basis for the stress-strain relation. Thus, the power-series expansion has terms in  $\epsilon^2, \epsilon^3, \epsilon^4, \dots$  where we require that the rate of damage must be positive for both positive and negative strains. The  $\epsilon^2$  term is the lowest-order term in the power-series expansion and will dominate for small strains. For large strains other terms may become important.

Substitution of eq. (1.3) into eq. (1.2) gives the strain  $\epsilon(t)$  in the damaged rod

$$\epsilon(t) = \frac{\sigma_0}{E_0[1 - \alpha(t)]}. \tag{3.3}$$

Combining eqs (3.2) and (3.3) we obtain

$$\frac{d}{dt}[1 - \alpha(t)] = -\frac{A \sigma_0^2}{E_0^2[1 - \alpha(t)]^2}. \tag{3.4}$$

Integrating with the initial condition  $\alpha(0) = 0$  we find

$$\alpha(t) = 1 - \left(1 - \frac{3A \sigma_0^2}{E_0^2} t\right)^{1/3}. \tag{3.5}$$

Substitution of eq. (3.5) into eq. (1.3) gives

$$E_{\text{eff}}(t) = E_0 \left(1 - \frac{3A \sigma_0^2}{E_0^2} t\right)^{1/3}. \tag{3.6}$$

Failure occurs at time  $t_f$  when  $E_{\text{eff}}(t_f) = 0$ , where  $\alpha(t_f) = 1$ ; thus we have

$$t_f = \frac{E_0^2}{3A \sigma_0^2}. \tag{3.7}$$

Substituting eq. (3.7) into eq. (3.5) we find

$$\alpha(t) = 1 - \left(1 - \frac{t}{t_f}\right)^{1/3}. \tag{3.8}$$

We obtain the time dependence of the effective Young modulus  $E_{\text{eff}}(t)$  by substituting eq. (3.7) into eq. (1.3) with the result

$$E_{\text{eff}}(t) = E_0 \left(1 - \frac{t}{t_f}\right)^{1/3}. \tag{3.9}$$

A similar derivation of this result has been given by Ben-Zion & Lyakhovsky (2002). This solution for the effective Young modulus

$E_{\text{eff}}(t)$  using the damage model is identical to the solution for the effective Young modulus obtained using the fibre-bundle model given in eq. (2.16) if we take  $\rho = 3$  in the hazard rate scaling relation eq. (2.7). The two totally independent approaches give identical results when we take  $\rho = 3$ .

Assuming  $\rho = 3$ , we equate the time to failure  $t_f$  given in eq. (2.10) for the fibre-bundle model to the time to failure  $t_f$  given in eq. (3.7) for the damage model with the result

$$A = \frac{E_0^2 v_0}{\sigma_0^2}. \quad (3.10)$$

The constant  $A$  in the damage rate equation (3.2) is related to the hazard rate  $v_0$  defined in eq. (2.7). With  $\rho = 3$  we have  $v_0 \propto \sigma_0^3$  from eq. (2.7), thus we have  $A \propto \sigma_0$  from eq. (2.10).

#### 4 GENERALIZED DAMAGE MODEL

In the previous section we showed that the equal load sharing fibre-bundle model and the damage model have identical solutions if  $\rho = 3$  in the hazard rate equation (2.7). Since the stress dependence of the hazard rate is solely empirical, the value  $\rho = 3$  has no particular meaning. Significantly,  $\rho = 3$  is typical of polycarbonate resins used in the manufacture of composite materials for which the fibre-bundle model was developed.

With  $\rho = 3$ , the damage variable  $\alpha(t)$  is equal to the fraction of failed fibres  $N_f(t)/N_0$  from eq. (3.1). This is not the case for other values of  $\rho$ . We now introduce a generalized definition of damage through the relation

$$E_{\text{eff}}(t) = E_0[1 - \alpha(t)]^{1/(\rho-2)}. \quad (4.1)$$

When  $\rho = 3$  this reduces to the standard definition of the variable given in eq. (1.3). Since we are modelling 1-D behaviour on a 3-D medium, we suggest that this generalization provides a phenomenological device for capturing the role played by the transverse dimensions.

An alternative generalization of the continuum damage theory has been given by Krajcinovic (1996, p. 477). Instead of introducing an arbitrary power into the basic definition of the damage variable as we have done in eq. (4.1), this author introduces an arbitrary power  $\epsilon^m(t)$  into the rate eq. (3.2). We prefer the generalization of eq. (1.3) as given in eq. (4.1) since we assume that the rate of damage is proportional to an even power of the strain.

Again we consider the failure of a rod under tension. Substitution of eq. (4.1) into eq. (1.2) gives the strain  $\epsilon(t)$  in the damaged rod

$$\epsilon(t) = \frac{\sigma_0}{E_0[1 - \alpha(t)]^{1/(\rho-2)}}. \quad (4.2)$$

Combining eqs (4.2) and (3.2) we find

$$\frac{d}{dt}[1 - \alpha(t)] = -\frac{A \sigma_0^2}{E_0^2[1 - \alpha(t)]^{2/(\rho-2)}}. \quad (4.3)$$

Integrating with the initial condition  $\alpha(0) = 0$ , we obtain

$$\alpha(t) = 1 - \left[1 - \frac{\rho A \sigma_0^2}{(\rho - 2) E_0^2} t\right]^{(\rho-2)/\rho}. \quad (4.4)$$

Substitution of eq. (4.4) into eq. (4.1) gives

$$E_{\text{eff}}(t) = E_0 \left[1 - \frac{\rho A \sigma_0^2}{(\rho - 2) E_0^2} t\right]^{1/\rho}. \quad (4.5)$$

Failure occurs at time  $t_f$  when  $E_{\text{eff}}(t_f) = 0$  [ $\alpha(t_f) = 1$ ], thus we have

$$t_f = \frac{(\rho - 2) E_0^2}{\rho A \sigma_0^2}. \quad (4.6)$$

Using eqs (4.6) and (4.4) we obtain

$$\alpha(t) = 1 - \left(1 - \frac{t}{t_f}\right)^{(\rho-2)/\rho}. \quad (4.7)$$

And the substitution of eq. (4.6) into eq. (4.5) gives eq. (2.16), the result obtained for the fibre-bundle model. Equating the time to failure given in eqs (2.10) and (4.6) we have

$$A = \frac{(\rho - 2) E_0^2 v_0}{\sigma_0^2}. \quad (4.8)$$

Using the generalized damage definition given in eq. (4.1) we recover the full fibre-bundle solution valid for arbitrary  $\rho$ .

Comparing eq. (2.17) with eq. (4.1), we obtain

$$\alpha(t) = 1 - \left[\frac{N(t)}{N_0}\right]^{\rho-2}. \quad (4.9)$$

When  $\rho = 3$  this reduces to eq. (3.1). For other values of  $\rho$ , eq. (4.9) gives the required dependence of  $\alpha(t)$  on  $N/N_0$ . In the general case, the damage variable  $\alpha$  is not simply proportional to the number of failed fibres as in eq. (3.1).

#### 5 TIME-DEPENDENT STRESS

In the above analysis we assumed that a force  $F_0$  was applied to a rod instantaneously at  $t = 0$ . We showed that the fibre-bundle model with  $\rho = 3$  and the damage model gave identical result. In order to test the generality of this correspondence further, we now consider the case in which the applied stress  $\sigma$  is a linearly increasing function of time

$$\sigma(t) = \beta t, \quad (5.1)$$

where  $\beta$  is a constant.

First we consider the fibre-bundle model. Again assuming equal load sharing so that eq. (2.6) is applicable, from eq. (5.1) the stress  $\sigma_f(t)$  in the remaining unbroken fibres is given by

$$\sigma_f(t) = \frac{N_0}{N(t)} \beta t. \quad (5.2)$$

Again we assume that the hazard rate is given by

$$v(t) = v_f \left[\frac{\sigma_f(t)}{\sigma(t_f)}\right]^\rho, \quad (5.3)$$

where  $v_f$  is the hazard rate at the failure stress  $\sigma(t_f)$ , which is given, from eq. (5.1), by

$$\sigma(t_f) = \beta t_f, \quad (5.4)$$

where  $t_f$  is again the failure time. Substitution of eq. (5.4) into eq. (5.3) gives

$$v(t) = v_f \left[\frac{\sigma_f(t)}{\beta t_f}\right]^\rho. \quad (5.5)$$

With this dependence of the hazard rate on stress there is a finite probability for the failure of fibres at all stress levels. There is no well-defined yield stress below which linear elasticity is applicable.

Combining eqs (2.1), (5.2) and (5.5) we have

$$\frac{dN(t)}{dt} = -v_f \left(\frac{t}{t_f}\right)^\rho \frac{N_0^\rho}{[N(t)]^{\rho-1}}. \quad (5.6)$$

Integrating with the initial condition  $N(0) = 0$ , we find

$$N(t) = N_0 \left[1 - \frac{\rho v_f t_f}{\rho + 1} \left(\frac{t}{t_f}\right)^{\rho+1}\right]^{1/\rho}. \quad (5.7)$$

Failure of the fibre-bundle occurs at  $t = t_f$  when  $N(t_f) = 0$ , the time to failure is given by

$$t_f = \frac{\rho + 1}{\rho v_f}. \quad (5.8)$$

Comparison of eq. (5.8) with eq. (2.10) shows that the time to failure for a linearly increasing stress is  $\rho + 1$  times the time to failure for a constant stress. The hazard rates  $v_0$  in eq. (2.10) and  $v_f$  in eq. (5.8) are equivalent since both apply at the time of failure.

Substitution of eq. (5.8) into eq. (5.7) gives

$$N(t) = N_0 \left[ 1 - \left( \frac{t}{t_f} \right)^{\rho+1} \right]^{1/\rho}. \quad (5.9)$$

Combining eqs (5.2), (5.4) and (5.9) we obtain

$$\sigma_f(t) = \sigma(t_f) \frac{t/t_f}{\left[ 1 - (t/t_f)^{\rho+1} \right]^{1/\rho}}. \quad (5.10)$$

Substitution of eq. (5.10) into eq. (2.12) gives the strain  $\epsilon_f(t)$  of each remaining fibre

$$\epsilon_f(t) = \sigma(t_f) \frac{t/t_f}{E_0 \left[ 1 - (t/t_f)^{\rho+1} \right]^{1/\rho}}. \quad (5.11)$$

And the effective Young modulus for the fibre-bundle is obtained by substituting eqs (5.11) and (5.4) into eq. (2.14)

$$E_{\text{eff}}(t) = E_0 \left[ 1 - \left( \frac{t}{t_f} \right)^{\rho+1} \right]^{1/\rho}. \quad (5.12)$$

Substitution of eq. (5.9) into eq. (5.12) again gives eq. (2.17). As in eq. (2.16), the effective Young modulus  $E_{\text{eff}}(t)$  decreases from its original value of  $E_{\text{eff}}(0) = E_0$  to  $E_{\text{eff}}(t_f) = 0$  at failure. This dependence is illustrated in Fig. 4 for  $\rho = 2-4$ . A comparison with Fig. 3 shows that damage develops much later when  $\sigma$  increases linearly with time than when it is instantaneously applied.

We now consider the damage model with an applied stress that increases linearly with time. From eqs (5.1) and (5.4) we have for  $t \leq t_f$

$$\sigma(t) = \sigma(t_f) \frac{t}{t_f}. \quad (5.13)$$

For a constant applied stress  $\sigma_0$  the damage parameter  $A$  defined in eq. (3.2) is a constant. The dependence of  $A$  on the hazard rate

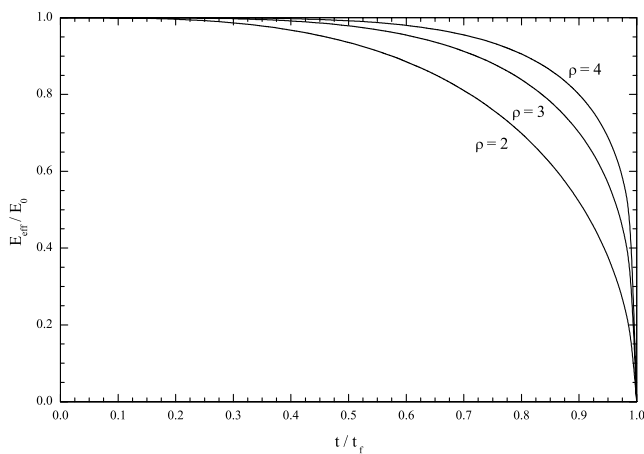


**Figure 4.** Dependence of the ratio of the effective Young modulus  $E_{\text{eff}}$  to the Young modulus of the undamaged material  $E_0$  on the time to failure  $t/t_f$  for  $\rho = 2-4$  from eq. (5.12). The force on the rod is a linearly increasing function of time starting at  $t = 0$ , failure of the rod occurs at  $t = t_f$ .

$v_0$  and  $\sigma_0$  has been given in eq. (3.10). For an applied stress that increases linearly with time we replace  $\sigma_0$  in eq. (3.10) with  $\sigma(t)$  as given by eq. (5.13). Furthermore, we replace  $v_0$  in eq. (3.10) with  $v(t)$ , which we obtain from eq. (5.3) taking  $\rho = 3$  and assuming  $v(t)$  is the damage rate at stress  $\sigma(t)$ . With these substitutions eq. (3.10) becomes

$$A(t) = \frac{E_0^2 v(t)}{\sigma^2(t)} = \frac{E_0^2 v_f}{\sigma^2(t)} \left[ \frac{\sigma(t)}{\sigma(t_f)} \right]^3 = \frac{E_0^2 v_f t}{\sigma^2(t_f) t_f}. \quad (5.14)$$

Substitution of eq. (5.14) into eq. (3.2) gives

$$\frac{d\alpha(t)}{dt} = \frac{v_f E_0^2 t}{\sigma^2(t_f) t_f} \epsilon^2(t). \quad (5.15)$$

And the substitution of eq. (5.13) into eq. (3.3) gives

$$\epsilon(t) = \frac{\sigma(t_f) t}{t_f E_0 [1 - \alpha(t)]}. \quad (5.16)$$

Using eq. (5.16), we are able to rewrite eq. (5.15) as follows

$$\frac{d\alpha(t)}{dt} = \frac{v_f}{[1 - \alpha(t)]^2} \left( \frac{t}{t_f} \right)^3. \quad (5.17)$$

Integrating with the initial condition  $\alpha(0) = 0$  we obtain

$$\alpha(t) = 1 - \left( 1 - \frac{3v_f t^4}{4t_f^3} \right)^{1/3}. \quad (5.18)$$

Failure occurs when  $\alpha(t_f) = 1$  so that

$$t_f = \frac{4}{3v_f}. \quad (5.19)$$

Combining eqs (1.3), (5.18) and (5.19) we obtain

$$E_{\text{eff}}(t) = E_0 \left[ 1 - \left( \frac{t}{t_f} \right)^4 \right]^{1/3}. \quad (5.20)$$

If we take  $\rho = 3$  we find eq. (5.19) is identical to eq. (5.8) and that eq. (5.20) is identical to eq. (5.12). Once again, we find that the fibre-bundle model and the damage model give identical results if  $\rho = 3$ . Thus, we see that the time-dependent stress model is a rescaled version of the constant stress model.

## 6 ACOUSTIC-EMISSION EVENTS

A characteristic of materials experiencing ‘damage’ are acoustic-emission events. For a solid material stressed beyond its elastic limit the acoustic-emission events are associated with microcracks. For a fibrous material the acoustic-emission events are associated with the failure of one or more fibres.

We now obtain an expression for the energy flux associated with the acoustic-emission events from a fibre-bundle as fibres break using the model considered above. In our fibre-bundle model we assume that individual fibres satisfy linear elasticity until failure. Thus the stored elastic energy in a single fibre  $e_f(t)$  at the time of failure is given by

$$e_f(t) = \frac{1}{2} V_f E_0 \epsilon_f^2(t), \quad (6.1)$$

where  $V_f$  is the volume of the fibre,  $E_0$  is the Young modulus of the fibre, and  $\epsilon_f$  is the strain in the fibre given by eq. (2.13). We assume that when a fibre fails, a fraction  $\eta_a$  of the stored elastic energy given by eq. (6.1) is the energy in the acoustic-emission event. The efficiency  $\eta_a$  is analogous to the seismic efficiency  $\eta_s$ , the fraction of the stored elastic energy lost during an earthquake that is radiated

in the seismic waves generated by earthquake. In both earthquakes and in acoustic-emission events from damaged materials, energy is also used to rupture material and in some cases is dissipated in frictional heating. We assume that the acoustic-emission efficiency  $\eta_a$  is a constant.

The rate at which energy is lost by acoustic-emission events is given by

$$\frac{de_{fa}(t)}{dt} = -\eta_a e_f(t) \frac{dN(t)}{dt}, \quad (6.2)$$

where  $e_{fa}(t)$  is the energy associated with the acoustic-emission event and  $e_f(t)$  is the stored elastic energy in a fibre. Substituting eq. (6.1) into eq. (6.2) we obtain

$$\frac{de_{fa}(t)}{dt} = -\frac{1}{2} \eta_a V_f E_0 \epsilon_f^2(t) \frac{dN(t)}{dt}. \quad (6.3)$$

Since the total volume of fibres is  $N_0 V_f$ , the rate of energy loss in acoustic-emission events per unit volume of material  $e_a(t)$  is given by

$$\frac{de_a(t)}{dt} = -\frac{1}{2} \eta_a \frac{E_0 \epsilon_f^2(t)}{N_0} \frac{dN(t)}{dt}. \quad (6.4)$$

From eq. (2.8), the rate at which fibres fail can be written

$$\frac{dN(t)}{dt} = -\frac{v_0 N_0^\rho}{[N(t)]^{\rho-1}} \quad (6.5)$$

and, from eqs (2.9) and (2.13), we have the fibre strain at its time of failure  $t$

$$\epsilon_f(t) = \frac{\sigma_0}{E_0} \frac{N_0}{N(t)}. \quad (6.6)$$

Using eqs (6.5) and (6.6), we can rewrite eq. (6.4) in the form

$$\frac{de_a(t)}{dt} = \frac{1}{2} \eta_a \frac{v_0 \sigma_0^2}{E_0} \left[ \frac{N_0}{N(t)} \right]^{\rho+1}. \quad (6.7)$$

Combining eqs (2.9), (2.10) and (6.7) we obtain

$$\frac{de_a(t)}{dt} = \frac{\eta_a v_0 \sigma_0^2}{2E_0} \frac{1}{(1-t/t_f)^{(\rho+1)/\rho}}. \quad (6.8)$$

This is the rate at which energy is radiated in acoustic-emission events during the failure of a fibre-bundle.

While the rate at which energy is lost in acoustic-emission events can be determined from the microscopic fibre-bundle model, this is not the case for the macroscopic damage model. We now use our analogue between the two models to determine a relationship between the energy addition associated with damage and the loss owing to acoustic-emission events.

We use the damage model to determine the rate at which work is being done on a rod. Since the stress on the rod  $\sigma_0$  is constant we have

$$\frac{dw(t)}{dt} = \sigma_0 \frac{d\epsilon(t)}{dt}, \quad (6.9)$$

where  $w(t)$  is the work per unit volume done on the rod. Taking the derivative of eq. (3.3) we obtain

$$\frac{d\epsilon(t)}{dt} = \frac{\sigma_0}{E_0 [1-\alpha(t)]^2} \frac{d\alpha(t)}{dt}. \quad (6.10)$$

Substitution of eqs (3.2), (3.3) and (6.10) into eq. (6.9) gives

$$\frac{dw(t)}{dt} = \frac{A \sigma_0^4}{E_0^3 [1-\alpha(t)]^4}. \quad (6.11)$$

Upon substitution of eqs (3.8) and (3.10) into eq. (6.11) we have

$$\frac{dw(t)}{dt} = \frac{v_0 \sigma_0^2}{E_0} \frac{1}{(1-t/t_f)^{4/3}}. \quad (6.12)$$

This result was also obtained by Ben-Zion & Lyakhovskiy (2002). Comparing eq. (6.12) with eq. (6.8), noting that  $\rho = 3$  in our analogue, we find that

$$\frac{de_a(t)}{dt} = \frac{\eta_a}{2} \frac{dw(t)}{dt}. \quad (6.13)$$

If the acoustic efficiency is  $\eta_a = 1$ , we find that one-half of the energy that is added to the damaged medium is lost in acoustic-emission events.

Next we determine the energy in acoustic-emission events when the applied stress is increasing linearly with time as given by eq. (5.1). Combining eqs (5.6) and (5.9), we obtain

$$\frac{dN(t)}{dt} = -\frac{v_f N_0 (t/t_f)^\rho}{[1 - (t/t_f)^{\rho+1}]^{(\rho-1)/\rho}}. \quad (6.14)$$

Using eqs (5.11) and (6.14), we can rewrite eq. (6.4) in the form

$$\frac{de_a(t)}{dt} = \frac{\eta_a v_f \sigma^2(t_f)}{2E_0} \frac{(t/t_f)^{\rho+2}}{[1 - (t/t_f)^{\rho+1}]^{(\rho+1)/\rho}}. \quad (6.15)$$

In the vicinity of a rupture we have  $t/t_f = 1 - \epsilon$  with  $\epsilon \ll 1$ . Thus we can write

$$\begin{aligned} [1 - (1 - \epsilon)^{\rho+1}]^{(\rho+1)/\rho} &\approx [1 - 1 + (\rho + 1)\epsilon]^{(\rho+1)/\rho} \\ &= [(\rho + 1)\epsilon]^{(\rho+1)/\rho} \end{aligned}$$

so that in this limit we obtain

$$\frac{de_a(t)}{dt} \propto \frac{1}{(1 - t/t_f)^{(\rho+1)/\rho}}. \quad (6.16)$$

Thus, the scaling in the vicinity of a rupture is the same as that obtained for the constant pressure result given in eq. (6.8).

We now compare the predicted acoustic-emission associated with material failure with experiments. Guarino *et al.* (1998, 1999) studied the failure of circular panels (220 mm diameter, 3–5 mm thickness) of chipboard and fibreglass. A differential pressure was applied across the panels until they failed. Acoustic-emission events were carefully monitored. For these relatively thin panels, bending stresses were negligible and the panels failed under tension (a mode I fracture). The acoustic-emission events were used to locate the associated microcracks. Initially, the microcracks appeared to be randomly distributed across the panel. As the pressure difference was increased, the microcracks localized in the region where the final rupture occurred. In the first series of experiments given by Guarino *et al.* (1998) the applied pressure difference (differential stress) was increased linearly with time in accordance with eq. (5.11).

These authors determined the cumulative energy associated with acoustic-emission events prior to rupture. The observed dependence of  $e_a/e_{tot}$  on  $(1 - P/P_f) = (1 - t/t_f)$  is given in Fig. 5(a) where  $e_a$  is the cumulative acoustic energy at time  $t$  and  $e_{tot}$  is the total acoustic energy at rupture ( $t = t_f$ ). Clear power-law behaviour is observed for  $(1 - t/t_f)$  less than approximately 0.1. The slope is  $e_a \propto (1 - t/t_f)^{-0.27 \pm 0.05}$ . This is equivalent to having  $de_a/dt \propto (1 - t/t_f)^{-1.27 \pm 0.05}$ . This result is in agreement with the predicted dependence given in eq. (6.16) if we take  $\rho = 3.7$ .

Guarino *et al.* (1998) also obtained a histogram for the frequency–magnitude statistics of the acoustic-emission events. For the

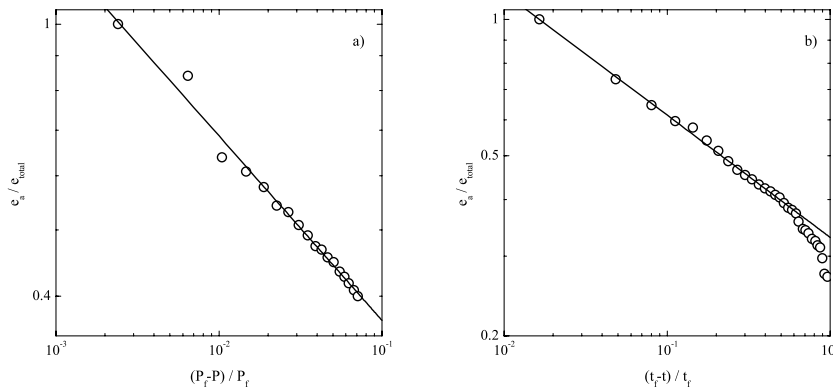


**Figure 5.** (a) Cumulative acoustic energy emissions  $e_a(t)$  divided by the total acoustic energy emissions  $e_{\text{tot}}$  at the time of rupture ( $t = t_f$ ) as a function of  $(P_f - P)/P_f$  where  $P$  is the applied pressure difference across the failing panel of chipboard and  $P_f$  is the pressure difference when the board fails. The applied pressure difference across the panel increased linearly with time in accordance with eq. (5.1). The straight-line correlation is with  $e_a \propto (1 - t/t_f)^{-0.27}$ . (b) Cumulative acoustic energy emissions  $e_a(t)$  at time  $t$  divided by the total acoustic energy emissions  $e_{\text{tot}}$  at the time of rupture ( $t = t_f$ ) as a function of  $(1 - t/t_f)$ . A constant pressure difference was applied at  $t = 0$ . The straight-line correlation is with  $e_a \propto (1 - t/t_f)^{-0.27}$  (Guarino *et al.* 1998, 1999).

chipboard panels they found that the number of events  $N_{\text{events}}$  with a given energy  $e_a$  satisfies the relation

$$N_{\text{events}} \propto e_a^{-\gamma} \quad (6.17)$$

with  $\gamma = 1.51 \pm 0.05$  for chipboard and  $\gamma = 2.0 \pm 0.1$  for fibreglass. For earthquakes, we have  $\gamma \approx \frac{5}{3}$ . A similar power-law distribution has also been found to be applicable for the fibre-bundles (Hemmer & Hansen 1992; Kloster *et al.* 1997).

Guarino *et al.* (1999) carried out a second series of experiments in which the applied pressure difference across the panel was increased instantaneously to a prescribed value and was held at that value until the circular panel failed. The cumulative energy associated with acoustic-emission events prior to rupture was determined. The observed dependence of  $e_a/e_{\text{tot}}$  on  $(1 - t/t_f)$  for these experiments is given in Fig. 5(b). Again a clear power-law behaviour is observed for  $(1 - t/t_f)$  less than approximately 0.5. Again the slope is  $e_a \propto (1 - t/t_f)^{-0.27}$ , which is equivalent to  $de_a/dt \propto (1 - t/t_f)^{-1.27}$ . This result is in agreement with the predicted dependence given in eq. (6.8) taking  $\rho = 3.7$ . The experiments find the same power-law behaviour for a constant applied pressure difference and for a pressure difference that is increasing linearly with time. This correspondence was also found in our analysis since the power-law dependence in eq. (6.8) is the same as the power-law dependence in eq. (6.16).

Although there is a scaling region in the acoustic-emission data that is in accord with our analysis, there are some aspects of the data that disagree with our analysis. The cumulative acoustic-emission energy can be obtained by integrating eq. (6.8). This result is not in agreement with the experimental data given in Fig. 5(b) for small times. We attribute this disagreement to the transition from random emission events at small times to self-organizing events as rupture is approached. Our analysis correctly predicts the self-similar scaling region near rupture.

## 7 SEISMIC ACTIVATION

Systematic increases in the intermediate level of seismicity prior to large earthquakes have been proposed by several authors (Sykes & Jaumé 1990; Knopoff *et al.* 1996; Jaumé & Sykes 1999). It has also been observed that there is a power-law increase in seismic activity prior to a major earthquake. This was first proposed by Bufe &

Varnes (1993). They considered the cumulative Benioff strain in a region defined as

$$\epsilon_B(t) = \sum_{i=1}^{N(t)} \sqrt{E_i}, \quad (7.1)$$

where  $E_i$  is the seismic energy release in the  $i$ th precursory earthquake and  $N(t)$  is the number of precursory earthquakes considered up to time  $t$ . Bowman *et al.* (1998) carried out a systematic study of the optimal spatial region and magnitude range to obtain power-law activation. Four examples of their results are given in Fig. 6. In each case  $\epsilon_B(t)$  has been correlated with the relation

$$\epsilon_B(t) = \epsilon_{\text{Bf}} - B \left(1 - \frac{t}{t_f}\right)^s, \quad (7.2)$$

where  $\epsilon_{\text{Bf}}$  is the cumulative Benioff strain when the large earthquake occurs,  $t_f$  is the time since the previous large earthquake, and  $B$  is a constant. For the four earthquakes illustrated in Fig. 6 it is found that  $s = 0.30$  (Kern County),  $s = 0.18$  (Landers),  $s = 0.28$  (Loma Prieta) and  $s = 0.18$  (Coalinga). Other examples of power-law seismic activation have been given by Bufe *et al.* (1994), Varnes & Bufe (1996), Brehm & Braile (1998, 1999), Robinson (2000) and Zöller *et al.* (2001).

Next we extend our acoustic-emission analysis to determine whether it is consistent with seismic activation. Using eq. (6.8), the rate of the Benioff strain associated with the fibre-bundle model is given by

$$\frac{d\epsilon_B(t)}{dt} = \sqrt{\frac{de_a(t)}{dt}} = \sqrt{\frac{\eta_a v_0}{2E_0}} \frac{\sigma_0}{(1 - t/t_f)^{(\rho+1)/2\rho}}. \quad (7.3)$$

The cumulative Benioff strain is given by

$$\epsilon_B(t) = \epsilon_{\text{Bf}} - \int_{\epsilon_B(t)}^{\epsilon_{\text{Bf}}} d\epsilon = \epsilon_{\text{Bf}} - \int_t^{t_f} \frac{d\epsilon_B(t)}{dt} dt. \quad (7.4)$$

Substituting eq. (7.3) into eq. (7.4) and integrating, we obtain

$$\epsilon_B(t) = \epsilon_{\text{Bf}} - \frac{\sigma_0(\rho - 1)}{2\rho} \sqrt{\frac{\eta_a v_0}{2E_0}} \left(1 - \frac{t}{t_f}\right)^{(\rho-1)/2\rho}. \quad (7.5)$$

Comparing eq. (7.5) with eq. (7.2), we see that the two equations are identical. Rundle *et al.* (2000) found that the distribution of values for the power-law exponent for 12 earthquakes was  $s = 0.26 \pm 0.15$ .



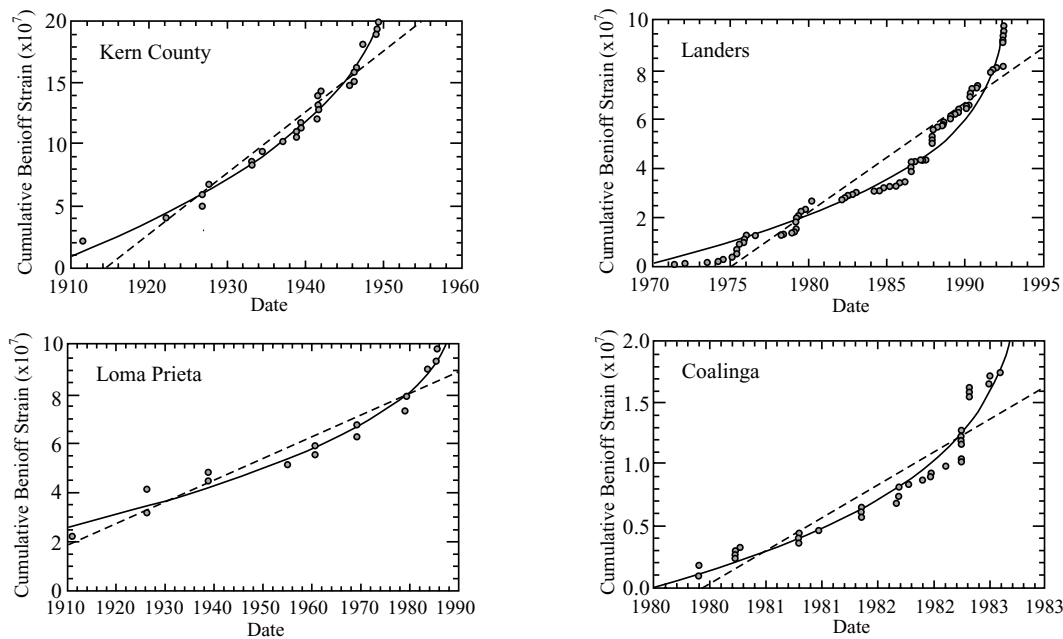


**Figure 6.** Power-law increase in the cumulative Benioff strain prior to four major earthquakes in California (Bowman *et al.* 1998). Each of the four examples has been correlated (solid line) with the power-law relation given in eq. (7.2). The dashed straight lines represent a best-fit constant rate of seismicity.

Comparing eq. (7.5) with eq. (7.2),  $s = 0.26$  corresponds to  $\rho = 2.1$ . For  $\rho = 3$  we find  $s = \frac{1}{3}$ , this result was previously obtained by Ben-Zion & Lyakhovskiy (2002).

## 8 DISCUSSION

Anelastic deformation of solids in engineering materials is often treated using continuum damage mechanics models. At the same time, statistical physicists have developed a variety of discrete models for material failure. In this paper, we show that two widely used models, a continuum, macroscopic damage model and a discrete, microscopic fibre-bundle model, yield identical solutions for a simple rupture problem.

The fibre-bundle model we consider is the dynamic time-to-failure model with uniform load sharing. The hazard rate defined in eq. (2.7) has a power-law dependence on stress  $\sigma(t)$  with exponent  $\rho$ . We consider the failure of a rod of material under tension. We consider two cases: (1) a constant tensional load is applied to the rod instantaneously and (2) the load increases linearly with time from zero. The solutions obtained using the continuum damage model are identical to the solutions obtained using the discrete fibre-bundle model if the stress exponent  $\rho = 3$ . We have generalized the damage model so that solutions agree with the fibre-bundle model for arbitrary values of  $\rho$ .

Guarino *et al.* (1998, 1999) studied the failure of circular panels of chipboard and fibreglass. They found that the cumulative energy associated with acoustic-emission events had a power-law dependence on the time to failure. We have shown that this dependence is in agreement with our solutions taking the power-law exponent  $\rho = 3.7$ . The power-law increase in acoustic emission is also consistent with the power-law increase in cumulative Benioff strain that has been recognized prior to a number of earthquakes (Bufe & Varnes 1993; Bowman *et al.* 1998).

The results given here raise a number of interesting questions regarding earthquake physics. The damage and fibre-bundle models considered in this paper yield results that are very analogous

to a second-order phase change. The power-law scaling is a characteristic of the approach to a phase change. However, material failure is a catastrophic event and is certainly not reversible. Phase changes involve a tuning parameter such as temperature or magnetic field.

Statistical physicists have related brittle rupture to liquid–vapour phase changes in a variety of ways. Buchel & Sethna (1997), Zapperi *et al.* (1997) and Kun & Herrmann (1999) associated brittle rupture with a first-order phase change. Alternatively, Andersen *et al.* (1997), Sornette & Andersen (1998) and Gluzman & Sornette (2001) argue that brittle rupture is analogous to a critical point (a second-order phase change). Newman & Knopoff (1982, 1983, 1990) and Knopoff & Newman (1983) used the dynamic renormalization group to explore how a hierarchy of failures—which they referred to as ‘crack fusion events’—could explain the relationship observed by Zhurkov (1965) relating the applied stress and the time to brittle failure. A number of authors have considered brittle rupture in analogue to spinodal nucleation (Selinger *et al.* 1991; Rundle *et al.* 1996, 1999, 2000; Zapperi *et al.* 1999). They draw an analogue between microcracking in a brittle solid and the nucleation of bubbles in a superheated liquid.

The relevance of the relatively simple models considered above to seismicity can be questioned, but we argue that the underlying physical processes are similar. In the models an increase in applied stress leads to ‘damage’ that weakens the material. Stress transfer is an important mechanism that leads to a power-law increase in the rate of failure. In the Earth’s crust there is a near steady-state rate of background seismicity, small earthquakes. These are equivalent to the random distribution of acoustic emissions observed in laboratory experiments. It is now widely accepted that there is an acceleration of intermediate level of seismicity prior to a major earthquake. This acceleration is also seen in the fibre-bundle model and damage models. It is attributed to the redistribution of stress in the material.

Time delays are inherent in both the fibre-bundle and damage models. Time delays are also observed in the Earth’s crust. Stress

transfer is associated with a major earthquake, there are regions in which this stress transfer results in an increase in stress. Subsequently, aftershocks occur in these regions. The time delays before aftershocks are analogous to the time delays in the models considered above.

## ACKNOWLEDGMENTS

The authors would like to thank Charlie Sammis and Robert Twiss for very helpful and constructive reviews. We would also like to thank Yehuda Ben-Zion, John Rundle, Bill Klein and Leigh Phoenix for many valuable and stimulating discussions. We take this opportunity to thank the National Science Foundation, whose financial support of the IMA programs made this collaborative research possible.

## REFERENCES

- Andersen, J.V., Sornette, D. & Leung, K.-T., 1997. Tricritical behaviour in rupture induced by disorder, *Phys. Rev. Lett.*, **78**, 2140–2143.
- Anifrani, J.-C., Le Floch, C., Sornette, D. & Souillard, B., 1995. Universal log-periodic correction to renormalization group scaling for rupture stress prediction from acoustic emissions, *J. Physique I*, **5**, 631–638.
- Bak, P. & Tang, C., 1989. Earthquakes as a self-organized critical phenomenon, *J. geophys. Res.*, **94**, 15 635–15 637.
- Ben-Zion, Y. & Lyakhovsky, V., 2002. Accelerated seismic release and related aspects of seismicity patterns on earthquake faults, *Pure appl. Geophys.*, **159**, 2385–2412.
- Ben-Zion, Y. & Rice, J.R., 1995. Slip patterns and earthquake populations along different classes of faults in elastic solids, *J. geophys. Res.*, **100**, 12 959–12 983.
- Bowman, D.D., Ouillon, G., Sammis, C.G., Sornette, A. & Sornette, D., 1998. An observational test of the critical earthquake concept, *J. geophys. Res.*, **103**, 24 359–24 372.
- Brehm, D.J. & Braile, L.W., 1998. Intermediate-term earthquake prediction using precursory events in the New Madrid seismic zone, *Bull. seism. Soc. Am.*, **88**, 564–580.
- Brehm, D.J. & Braile, L.W., 1999. Intermediate-term earthquake prediction using the modified time-to-failure method in Southern California, *Bull. seism. Soc. Am.*, **89**, 275–293.
- Buchel, A. & Sethna, J.P., 1997. Statistical mechanics of cracks: fluctuations, breakdown, and asymptotics of elastic theory, *Phys. Rev. E*, **55**, 7669–7690.
- Bufe, C.G. & Varnes, D.J., 1993. Predictive modeling of the seismic cycle of the greater San Francisco Bay region, *J. geophys. Res.*, **98**, 9871–9883.
- Bufe, C.G., Nishenko, S.P. & Varnes, D.J., 1994. Seismicity trends and potential for large earthquakes in the Alaska–Aleutian region, *Pure appl. Geophys.*, **142**, 83–99.
- Coleman, B.D., 1956. Time dependence of mechanical breakdown phenomena, *J. appl. Phys.*, **27**, 862–866.
- Coleman, B.D., 1958. Statistics and time dependence of mechanical breakdown in fibers, *J. appl. Phys.*, **29**, 968–983.
- Curtin, W.A., 1991. Theory of mechanical properties of ceramic-matrix composites, *J. Am. Ceram. Soc.*, **74**, 2837–2845.
- Freund, L.B., 1990. *Dynamic Fracture Mechanics*, Cambridge University Press, Cambridge.
- Gluzman, S. & Sornette, D., 2001. Self-consistent theory of rupture by progressive diffuse damage, *Phys. Rev. E*, **63**, 066 129.
- Guarino, A., Garcimartin, A. & Ciliberto, S., 1998. An experimental test of the critical behavior of fracture precursors, *Eur. Phys. J. B*, **6**, 13–24.
- Guarino, A., Ciliberto, S. & Garcimartin, A., 1999. Failure time and microcrack nucleation, *Europhys. Lett.*, **47**, 456.
- Hemmer, P.C. & Hansen, A., 1992. The distribution of simultaneous fiber failures in fiber-bundles, *J. appl. Mech.*, **59**, 909–914.
- Hirata, T., Satoh, T. & Ito, K., 1987. Fractal structure of spatial distribution of microfracturing in rock, *Geophys. J. R. astr. Soc.*, **90**, 369–374.
- Jaumé, S.C. & Sykes, L.R., 1999. Evolving towards a critical point: a review of accelerating seismic moment/energy release prior to large and great earthquakes, *Pure appl. Geophys.*, **155**, 279–306.
- Johansen, A. & Sornette, D., 2000. Critical ruptures, *Eur. Phys. J. B*, **18**, 163–181.
- Kachanov, L.M., 1986. *Introduction to Continuum Damage Mechanics*, Martinus Nijhoff, Dordrecht.
- Kloster, M., Hansen, A. & Hemmer, P.C., 1997. Burst avalanches in solvable models of fibrous materials, *Phys. Rev. E*, **56**, 2615–2625.
- Knopoff, L. & Newman, W.I., 1983. Crack fusion dynamics: a model for large earthquakes, *Pure appl. Geophys.*, **121**, 495–510.
- Knopoff, L., Levshina, T., Keilis-Borok, V.I. & Mattoni, C., 1996. Increased long-range intermediate-magnitude earthquake activity prior to strong earthquakes in California, *J. geophys. Res.*, **101**, 5779–5796.
- Krajcinovic, D., 1996. *Damage Mechanics*, Elsevier, Amsterdam.
- Kun, F. & Herrmann, H.J., 1999. Transition from damage to fragmentation in collision of solids, *Phys. Rev. E*, **59**, 2623–2632.
- Lemaitre, J. & Chaboche, J.-L., 1990. *Mechanics of Solid Materials*, Cambridge University Press, Cambridge.
- Lockner, D.A., 1993. The role of acoustic emissions in the study of rock fracture, *Int. J. Rock. Mech. Min. Sci. Geomech. Abs.*, **7**, 883–889.
- Lyakhovsky, V., Podladchikov, Y. & Poliakov, A., 1993. A rheological model of a fractured solid, *Tectonophysics*, **226**, 187–198.
- Lyakhovsky, V., Ben-Zion, Y. & Agnon, A., 1997. Distributed damage, faulting and friction, *J. geophys. Res.*, **102**, 27 635–27 649.
- Mogi, K., 1962. Study of elastic shocks caused by the fracture of heterogeneous materials and its relations to earthquake phenomena, *Bull. Earthq. Res. Inst.*, **40**, 125–173.
- Newman, W.I. & Knopoff, L., 1982. Crack fusion dynamics: a model for large earthquakes, *Geophys. Res. Lett.*, **9**, 735–738.
- Newman, W.I. & Knopoff, L., 1983. A model for repetitive cycles of large earthquakes, *Geophys. Res. Lett.*, **10**, 305–308.
- Newman, W.I. & Knopoff, L., 1990. Scale invariance in brittle fracture and the dynamics of crack fusion, *Int. J. Fracture*, **43**, 19–24.
- Newman, W.I. & Phoenix, S.L., 2001. Time dependent fiber-bundles with local load sharing, *Phys. Rev. E*, **63**, 021 507.
- Otani, H., Phoenix, S.L. & Petrina, P., 1991. Matrix effects on lifetime statistics for carbon fibre–epoxy microcomposites in creep rupture, *J. Mat. Sci.*, **26**, 1955–1970.
- Robinson, R., 2000. A test of the precursory accelerating moment release model on some recent New Zealand earthquakes, *Geophys. J. Int.*, **140**, 568–576.
- Rundle, J.B., Klein, W. & Gross, S., 1996. Dynamics of a traveling density wave model for earthquakes, *Phys. Rev. Lett.*, **76**, 4285–4288.
- Rundle, J.B., Klein, W. & Gross, S., 1999. Physical basis for statistical patterns in complex earthquake populations: models, predictions and tests, *Pure appl. Geophys.*, **155**, 575–607.
- Rundle, J.B., Klein, W., Turcotte, D.L. & Malamud, B.D., 2000. Precursory seismic activation and critical point phenomena, *Pure appl. Geophys.*, **157**, 2165–2182.
- Selinger, R.L.B., Wang, Z.G., Gelbart, W.M. & Ben-Shaul, A., 1991. Statistical–thermodynamic approach to fracture, *Phys. Rev. A*, **43**, 4396–4400.
- Smith, R.L. & Phoenix, S.L., 1981. Asymptotic distributions for the failure of fibrous materials under series-parallel structure and equal load-sharing, *J. appl. Mech.*, **48**, 75–82.
- Sornette, D. & Andersen, J.V., 1998. Scaling with respect to disorder in time-to-failure, *Eur. Phys. J. B*, **1**, 353–357.
- Sykes, L.R. & Jaumé, S.C., 1990. Seismic activity on neighboring faults as a long-term precursor to large earthquakes in the San Francisco Bay region, *Nature*, **348**, 595–599.
- Turcotte, D.L., 1999. Seismicity and self-organized criticality, *Phys. Earth planet. Inter.*, **111**, 275–293.
- Varnes, D.J. & Bufe, C.G., 1996. The cyclic and fractal seismic series preceding an  $m_b = 4.8$  earthquake on 1980 February 14 near the Virgin Islands, *Geophys. J. Int.*, **124**, 149–158.

- Zapperi, S., Ray, P., Stanley, H.E. & Vespignani, A., 1997. First-order transition in the breakdown of disordered media, *Phys. Rev. Lett.*, **78**, 1408–1411.
- Zapperi, S., Ray, P., Stanley, H.E. & Vespignani, A., 1999. Avalanches in breakdown and fracture processes, *Phys. Rev. E*, **59**, 5049–5057.

- Zhurkov, S.N., 1965. Kinetic concept of strength of solids, *Int. J. Fracture Mech.*, **1**, 311–323.
- Zöller, G., Hainzl, S. & Kurths, J., 2001. Observation of growing correlation length as an indicator for critical point behavior prior to large earthquakes, *J. geophys. Res.*, **106**, 2167–2175.